Twist Propagation in Hα Surges

Patricia Jibben and Richard C. Canfield

Physics Department, Montana State University, Bozeman, MT 59717-3840

jibben@mithra.physics.montana.edu

canfield@physics.montana.edu

ABSTRACT

We have studied Mees Solar Observatory Hα spectroheliogram and Doppler velocity movies of surges in 11 active regions. We used these movies to observe the surges' rotating motion, direction of propagation, and implied handedness of that motion. We were able to co-register movies containing 47 surges with Haleakala Stokes Polarimeter vector magnetograms. We could hence determine the direction of twist stored in the magnetic field at the point of origin of each surge. We found (with a 99% confidence) that the direction of observed spin of these surges is consistent with the relaxation of the stored twist in the magnetic field. Magnetic reconnection of twisted flux tubes with their less-twisted surroundings can account for the production and rotating motion of these surges.

Subject headings: Sun: activity, magnetic fields, sunspots

1. Introduction

Surges are straight or slightly curved ejections that reach peak velocities of 50-200 km s^{-1} (Svestka 1976). These ejections are called "sprays" when they are faster, brighter and flare-related (Roy 1973). Both spectroscopy (Xu, Ding, & Yin 1984; Gu et al. 1994; Canfield et al. 1996) and imaging (Gaizauskas & Kerton 1992) reveal torsional motion along the trajectory of ascent that typically lasts 10-30 minutes. Surges take place in the lower chromosphere and can reach heights of 200 Mm into the corona. The surge material either fades or returns into the chromosphere along the trajectory of ascent (Tandberg-Hanssen 1977; Foukal 1990). Surges show homology, pulsing behavior, and occur at the boundaries of magnetic field concentrations (Roy 1973). They are associated with satellite sunspots (Bumba 1960; Rust 1968) and moving magnetic features (Gaizauskas 1983). Sunspot growth and evolution (e.g. decay) are both important factors in the production of surges (Roy 1973; Gaizauskas 1996).

Both Rust (1968) and Roy (1973) proposed that reconnection of magnetic fields near a coronal neutral point above satellite spots accounts for surges. After a surge occurs a relaxation of the boundary (neutral line) between two regions of opposite polarity may be seen (Roy 1973). Kurowaka & Kawai (1993) showed that surges are seen in the early stages of flux emergence and concluded that they are produced by magnetic reconnection between the emerging flux region and the preexisting surrounding region.

Xu et al. (1984) proposed that the surges' rotating motion is generated by double pole diffusion of plasma due to a sharp density gradient between the surge material and surrounding corona. Gu et al. (1994) suggest magnetic reconnection causes the mass ejection but they agree with Xu et al. in that double pole diffusion causes the surge to rotate. Canfield et al. (1996) attributed the rotating motion to the redistribution of stored twist after reconnection of field lines with different values of twist density (turns per unit length). In this paper, we test the latter explanation. We examine the relationship between surge spin and the stored twist in the magnetic field using Hα spectroheliograms and vector magnetograms. We show that magnetic reconnection of twisted flux tubes with their less-twisted surroundings can account for both the production and rotating motion of the observed surges.

2. Instrumentation

The Mees Solar Observatory data consists of digital Hα spectroheliograms from the Mees CCD Imaging Spectrograph (MCCD; Penn et al. 1991) and vector magnetograms from the Haleakala Stokes Polarimeter (HSP; Mickey 1985). The MCCD obtains digital spectroheliograms in the spectral range Hα $\pm$10 Å by scanning the solar image from a 25 cm Coudé coronagraph telescope across a spectrograph slit. All pixels in the spectral dimension and one spatial dimension (along the spectrograph slit, terrestrial north-south) are sampled simultaneously; the other spatial dimension is built up sequentially. The resultant data sets have 2.3″ pixel^{-1} spatial and $\approx$ .37 Å pixel^{-1} spectral resolution across a field of view ranging from 108″ $\times$ 117″ to 230″ $\times$ 290″ depending on the details of the observing sequence.

The HSP provides simultaneous Stokes I, Q, U, and V profiles of the spectral lines Fe I $\lambda\lambda$ 6301.5 and 6302.5 Å. Magnetograms are obtained by a rectangular raster scan over the target active region. All pixels in the spectral dimension are sampled simultaneously and the two spatial dimensions are built up sequentially, with a typical scan time of an hour. At each raster point the strength of the magnetic field parallel (B_l) and transverse (B_t) to the line of sight, and the azimuth ϕ of the transverse field, are determined by one of two methods depending on the fractional polarization. When the polarization is $\geq 1\%$ (corresponding to a field strength $\gtrsim$ 100 G) a nonlinear least-squares fit of theoretical Stokes profiles (Unno 1956;

Rachkovsky 1962) is performed on both Fe I lines using the computer code of Skumanich & Lites (1987). In low-field regions the flux is determined using integrated properties of the Stokes Profiles (Ronan, Mickey, & Orrall 1987). Faraday rotation and magnetic filling factor are taken into account in the manner described by those authors.

3. Observations

Surges are not a common phenomenon on the sun, although they are one of the more dramatic forms of plasma ejection. Not all active regions produce surges, and very few produce a sizeable number. Several criteria were used to determine whether an active region might produce surges, and therefore be selected for our study. Roy (1973) observed surges were more likely to occur in regions of evolving magnetic features and significant flux change over a period of a day. The changing area of an active region is a good indication of emerging flux or decaying flux. Active regions whose area was changing ($\Delta a/a \geq 10\%$ between consecutive days) were considered. The daily value for the area was obtained from the NOAA Active Region Summaries published in Solar-Geophysical Data.

Sammis, Tang & Zirin (2000) showed that active regions with an area greater than 1000 μh [1] and classified $\beta\gamma\delta$ are unusually active. Therefore, our study also focused on active regions that were classified either δ or $\beta\gamma\delta$ by the Mt. Wilson magnetic classification scale, and had relatively large areas ($a \geq 500\mu$h.) To be included in our study, the active regions had to be well sampled with both the MCCD and the HSP. Finally, we required that the active region be within $\pm$ 45 degrees of the central meridian; this reduces the uncertainty in resolution of the 180 degree azimuth ambiguity in the HSP data (Canfield et. al 1993.)

Table 1 is a list of all active regions that we studied, along with the number of surges observed. Certain regions stand out because they produced a large number of surges. It is interesting that these regions have quite diverse properties. Active regions AR7260 and AR7590 were both classified $\beta\gamma\delta$ and had large areas that significantly changed from day to day. Both regions actively produced surges and followed the criteria well. The active region AR7117 didn't fit all of the criteria, but it grew rapidly and several days of data were available. It is classified as β and has a relatively small area. It also produced a large amount of surges. AR6891 however, didn't. It fit all of the criteria, produced many flares, but produced few surges in comparison to the others. The criteria we applied will not guarantee that an active region will produce surges, but are a useful set of guidelines with which to chose regions to study.

[1] 1 μh is one millionth of the visible disk of the Sun.

3.1. Hα Spectroheliograms and Doppler Shifts

MCCD movies were created from sequential spectroheliograms at 15-30 second intervals. The movie frames (Figure 1) display Hα line center intensity (right panel) and simultaneous Doppler Velocity (left panel). To maximize our Doppler-velocity sensitivity, we apply to the spectra Fourier filtering, interpolation, and padding with zeros at the Nyquist frequency. We then fit the core of the Hα line profile with a parabola. From the shifts of the minima of the fitted profiles of each pixel, we construct Doppler velocity maps; from the intensity of the minima of each pixel we construct line-center spectroheliograms. Figure 1 shows one frame of the MCCD movie for NOAA AR7117 taken 1992 March 28. The arrow points out an observed surge. All the surges observed had some sort of rotational motion associated with them indicated by red shift on one side of the surge, blue shift on the other, as seen in the Doppler velocity display. The rotational velocity of the surge in Figure 1 is on the order of 10^{-3} radian s^{-1}, and the velocity at which is elongates is 150 km s^{-1}. This value of the rotational velocity is consistent with previous work by Xu et al. (1984), Gu et al. (1994), and Canfield et al. (1996). The last three columns of Table 1 refer to the surge handedness, which is defined from the relationship between the direction of translational motion along the surge axis and the rotational motion around it. In all, 396 surges were observed; of these, handedness could be determined in 249. Figure 2 demonstrates how the handedness of a surge was determined from successive frames. It clearly shows that the surge is propagating towards the left and spinning clockwise as viewed from its point of origin. The surge motion was therefore classified as right-handed.

Surges come in many different shapes and sizes, but a common attribute is that they appear to rotate. However, the rotating motions vary. In most cases the surges' spin is consistent throughout its lifetime. However, we observed several cases in which the handedness of motion abruptly changed as well as cases in which 2 or more surges take place simultaneously. Some surges appeared to fall back in on themselves while others seemed to be obliterated by some unseen force and then change their rotational motion. Such surges could not be assigned a definite handedness and were not included in our study.

About half of the active regions that were studied were located in the northern hemisphere of the sun. If the Coriolis force plays some rule, however indirect, we expect to find a hemispheric preference for surge handedness. The ϕ coefficient (Daniel 1990) is designed for evaluation of statistical significance in studies using variables (e.g., handedness) that can take on only one of two mutually exclusive values. This coefficient is related to chi-squared values through $\chi^2 = n\phi$, where n is the total number observed surges. This can be compared to tabulated chi-square values with 1 degree of freedom. A truth table for Hα surges and hemisphere preference is given in Table 2. For this dataset, we find that $\chi^2 = 0.9924$ which

corresponds to a 68% correlation between surge handedness and the hemisphere of the sun where the surge occurred. If a hemispheric preference for surge spin exists, our dataset is far too small to show it.

3.2. HSP Vector Magnetograms and α Maps

We used the two standard types of Haleakala Stokes Polarimeter vector magnetograms (Canfield et al. 1993) *i.e.*, half-resolution (5.6" pixel spacing) and full-resolution (2.8" pixel spacing). The twist stored in the magnetic field was measured in terms of the force-free field parameter α, where

$$\nabla \times \mathbf{B} = \alpha \mathbf{B}. \tag{1}$$

We computed α from the z-component of equation (1).

$$\alpha B_z = \mu J_z = (\nabla \times B)_z. \tag{2}$$

where B_z is the vertical magnetic field strength (flux density), J_z is the vertical current density (both in a heliographic coordinate system), and $\mu = 4\pi \times 10^{-3}$ G m A^{-1}. We resolved the 180° azimuth ambiguity of the transverse field B_{trans} and computed J_z using the techniques described by Canfield et al. (1993). The noise level in the original magnetograms is usually not more than about 100 G for transverse fields and 10 G for longitudinal ones. To take into account variations from one magnetogram to the next, the 1 σ noise level of J_z was calculated for every magnetogram using a histogram of J_z values. We then analyzed α only for pixels for which $B_{trans} > 300$ G and $J_z > \sigma_{J_z}$. Such α maps show the spatial distribution of twist ($\alpha > 0$ where the fields are right-handed.) Figure 3 shows a vector magnetogram and a corresponding α map for one of the studied active regions, superimposed on the white light image at the time of observation. The α map shown is typical, in the sense that there is a complex pattern in which patches of strong twist of opposite handedness are near one another (Pevtsov, Canfield & Metcalf 1994). These authors found that this pattern lasts much longer (27 hours) than the time to complete a magnetogram. For the present purposes, we are interested only in the sign of α. For this reason we pick the contour in Figures 3 and 4 at an empirically determined fraction (87.5%) of the maximum unsigned α value for each map. This procedure ensures contours enclose all contiguous α values of a given sign.

The best-fit single value α_{best} was determined for the whole active region using the method described by Pevtsov, Canfield & Metcalf (1995). The ϕ coefficient was used to test for significance between α_{best} for an active region and surge handedness. Of the 249 surges observed with definite handedness, 127 were observed in active regions where α_{best} could be calculated. Table 3 is the truth table for this analysis. The $\chi^2 = 0.9382$ which corresponds

to a 67% probability these are related. If the handedness of surges depends on the overall twist (α_{best}) of their parent active region, our dataset is far too small to show it.

3.3. MCCD and HSP Co-registration

We co-registered the MCCD and HSP data using white light images and a least-squares method based on feature recognition. From the residuals we conclude that the accuracy of this co-registration is typically a few arc seconds. The contours of α were placed over the Doppler velocity movies based on the white light co-registration. The start sequence for the magnetograms fell within a few minutes of the start sequence for the MCCD data. The start times for the two data sets were never more than 3 hours apart. This time difference is about an order of magnitude shorter than the time scale for evolution of the α patterns found by Pevtsov et al., so we can safely ignore it.

Figure 4 is one frame of a co-registered movie. The surge originated at the boundary of a region of negative α value, meaning the photospheric magnetic field was twisted in a left handed sense. The origin of the surge was determined either by identifying the base of the surge when it first appeared or identifying the point where the surge disappeared after it fell back down into the chromosphere. The arrow in Figure 4 points to the location associated with surge. The area encompasses several pixels and coincides with a redshift region when the surge is launched. In this case, the redshift patch is associated with only a single α contour, which we identify with its origin.

The area scanned with the HSP is typically smaller than scanned with the MCCD, and α contours can be determined in only a fraction of the HSP scanned area because of low signal relative to noise. Of all the observed surges, only 47 had points of origin that could be identified with a measured α value in a magnetogram. Furthermore, it was not possible to determine the handedness of all of these 47 surges. Table 4 lists all 26 surges for which we could determine both the handedness of the surge and the sign of α at its point of origin. Most of the surges did not occur deep within an α contour; on the contrary, they tended to occur near the edge of a sunspot and near a boundary separating opposite signs of α. Of course, this is a source of uncertainty in determination of the sign of α at the point of origin of each surge. In this study we simply decided which sign of α was preferred for each event. That is to say, the region of origin seemed to have more area on one side of the boundary vs the other.

Through a statistical analysis, are we able to overcome this uncertainty. The dataset of 26 surges with known handedness of motion in Hα and in the magnetic field of the

photosphere, shown in Table 5, appears to show a correlation. The same statistical analysis discussed earlier (Daniel 1990) was used here. For the dataset of Table 5 we find that $\chi^2 = 6.635$, which means that in this data set there is a correlation between the stored twist in the magnetic field at the point of origin and handedness of the surge spin at the 99% confidence level.

4. Interpretation

We believe magnetic reconnection of twisted magnetic flux with less twisted (relaxed) flux explains the correlation discussed above. We hold this view for two reasons. First, we would expect that energy release will accompany reconnection, and brightenings are a common feature of the observed events. Second, if the reconnected field lines do not have the same twist per unit length, post-reconnection twist propagation will take place, as discussed below.

Figure 5 is a cartoon model of post-reconnection twist propagation in a straight thin flux tube with a rigid lower boundary (photosphere) and an open upward boundary (corona). This model assumes twist propagates as a torsional Alfvén wave. Magnetic reconnection is assumed to take place at time 1 at point a, between a region that is twisted in a left handed sense and one that is not. The left column in figure 5 demonstrates how the two waves interact through time. The dashed line is the twist per unit length ($d\theta/dz$) while the solid line is the twist per unit time ($d\theta/dt$). The right-hand column shows the rotational motion and stored twist in the magnetic field. The twist per length is shown as red or blue shifts (white or black) and the twist per time is shown as twisted lines. Initially, there is no rotational motion, although the left-hand twist can be seen. At time 2, twist is spreading outward symmetrically from point a. At this instant, some untwisting can be seen in the intermediate region. In that region the Doppler shift can be seen and an intermediate left-handed twist can be seen. The intermediate twisted regions continues to grow until the left-hand side hits the lower boundary (rigid wall). At this time, the twisted region is deflected and propagates rightward at the Alfvén speed as in instants 3 and 4. Now both regions above and below the surge are relaxed and the twist that was stored in the magnetic field has been released. A two dimensional view of this is given in Figure 6 where a small left-handed twisted dipole is reconnecting with the untwisted large-scale field at X. Twist in section N-X goes to the large scale field, that in section S-X goes to small loop formed near S. The arrow above X indicates a clockwise motion, as viewed from the reconnection site, creating a right-handed surge.

We conclude that magnetic reconnection of twisted flux tubes with their surroundings

can account for the production and rotational motion of observed surges.

5. Acknowledgments

Many thanks to Dana Longcope, Alexei Pevtsov, Alisdair Davey, Kevin Reardon and the observing staff of Mees Solar Observatory. This research has been supported by NASA SR&T grants NAG5-6110 and NAG5-11873.

REFERENCES

Bumba, V. 1960, Publ. Crim.Astrophys. Obs., 23, 212

Canfield, R.C., De La Beaujardiére, J.-F., Fan, Y., Leka, K.D., McClymont, A.N., Metcalf, T.R., Mickey, D.L., & Wülser, J.-P. 1993, ApJ, 411, 362

Canfield, R.C., Reardon, K.P., Leka, K.D., Shibata, K., Yokoyama, T., Shimojo, M. 1996, ApJ, 464, 1016

Daniel, W. 1990, Applied Nonparametric Statistics, (2d ed.; Boston:PWS-Kent Publishing Company)

Foukal, P. 1990, Solar Astrophysics, (New York:Wiley), 354

Gaizauskas, V. 1983, in Adv. Space Res., Vol. 2, No. 11, 11

Gaizauskas, V. 1996, Sol. Phys., 169, 357

Gaizauskas, V., & Kerton, C.R. 1992, in IAU Colloq. 133, Eruptive Solar Flares ed. Z. Svestka, B.V. Jackson, & M.E. Machado (Berlin:Springer-Verlag), 347

Gu, X.M., Lin, J., Li, K.L., Xuan, J.Y., Luan, T., & Li, Z.K. 1994, A&A, 282, 240

Kurowaka, H., & Kawai, G. 1993, in ASP Conf. Ser., 46, The Magnetic and Velocity Fields of Solar Active Regions, ed. H. Zirin, G. Ai, & H. Wang (San Francisco:ASP), 507

Mickey, D. L. 1985, Sol. Phys., 97, 223

Penn, M.J., Mickey, D.L., Canfield, R.C., & LaBonte, B.J. 1991, Sol. Phys., 135, 163

Pevtsov, A.A., Canfield, R.C., & Metcalf, T.R. 1994, ApJ, 425, L117

Pevtsov, A.A., Canfield, R.C., & Metcalf, T.R. 1995, ApJ, 440, L109

Rachkovsky, D.N. 1962, Izv. Krymsk. Astrofiz. Obs., 27, 148

Ronan, R.S., Mickey, D.L., & Orrall, F.Q. 1987, Sol. Phys., 113, 353

Roy, J.-R. 1973, Sol. Phys., 28, 95

Rust, D. M. 1968, IAU Symp., 35, Structure and Development of Solar Active Regions, ed. K. O. Kiepenheuer (Dordrecht: Reidel), 77

Sammis, I., Tang, F., & Zirin, H. 2000, Apj, 540, 583

Skumanich, A., & Lites, B.W. 1987, ApJ, 322, 473

Svestka, Z. 1976, Solar Flares (Dordrecht:Reidel)

Tandberg-Hanssen, E. 1977, Illustrated Glossary for Solar and Solar-Terrestrial Physics, ed. A. Bruzek & C. J. Durrant (Dordrecht:Reidel), 106

Unno, W. 1956, PASJ, 8, 108

Xu, A., Ding, J., & Yin, S. 1984, Acta. Astron. Sin, 25, 119

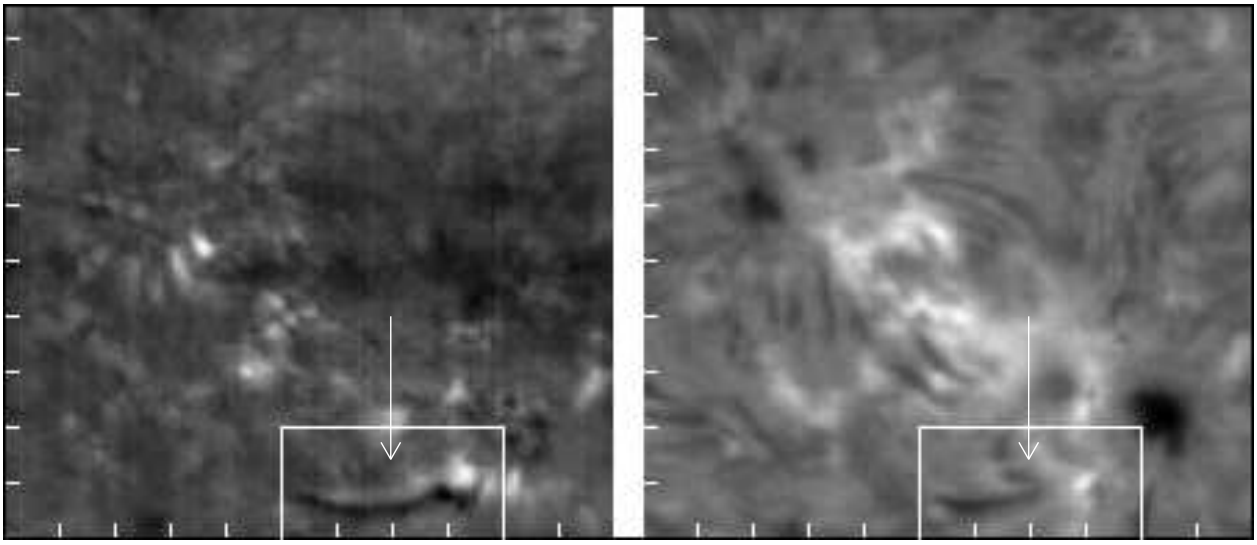

Fig. 1.— A single frame of a typical MCCD spectroheliogram movie at the time of a surge (arrow). AR7117 (N6E2), 1992 March 28, start time 21:57:20 UT. Scale: Tick mark spacing 23.3" Orientation: In this and all subsequent figures Earth North is up, East to the left. Left: Hα Doppler velocity. In this and all subsequent figures white indicates red shift, black – blue shift. Right: Hα line center intensity. The arrow points to a surge after it has elongated.

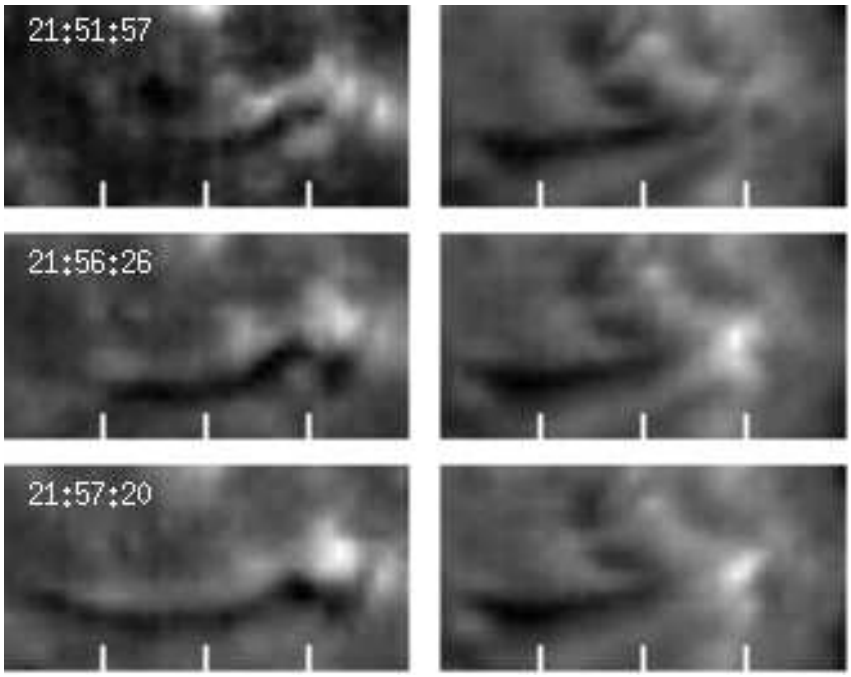

Fig. 2.— Boxed region from Figure 1. This series of Hα line-center spectroheliograms (right) and velocity maps (left) shows that the surge is propagating to the left and is rotating clockwise as viewed from its point of origin. Its motion is defined to be right-handed.

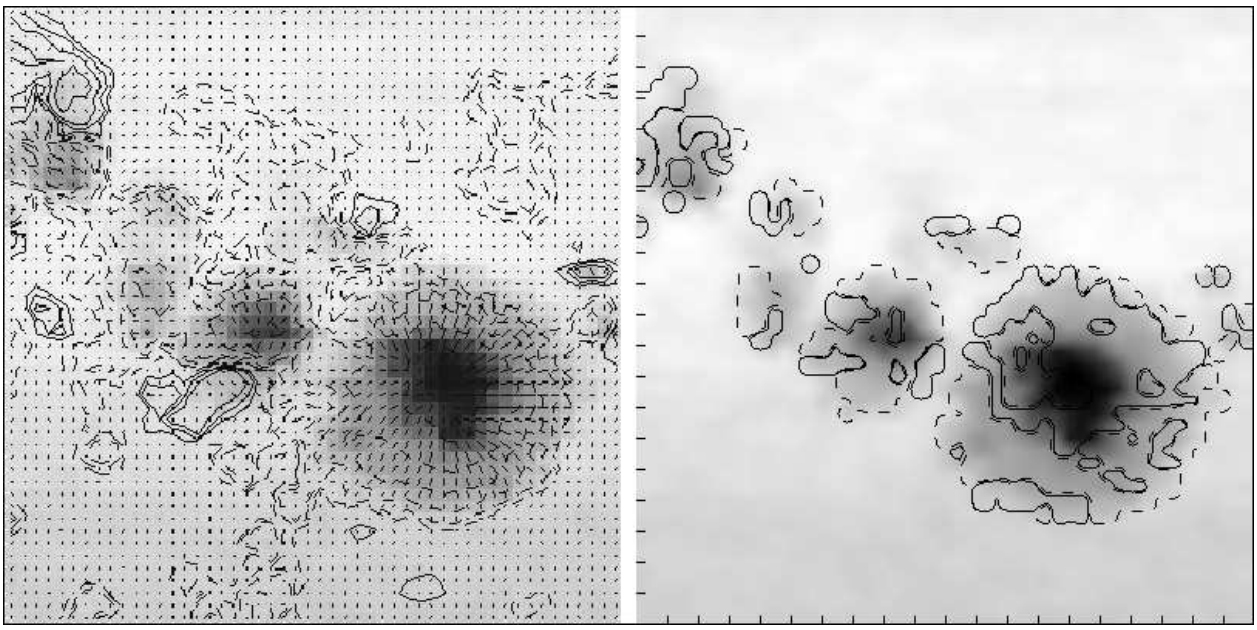

Fig. 3.— AR7117. Left: vector magnetogram made on 1992 March 28 from 21:12:01-22:43:43 UT. Contours of negative longitudinal magnetic flux B_l are dashed, positive B_l are solid. B_l contour levels: ± 50, 100, 200, 400, 600, 1600, 3200 G. Pixel spacing is $2.6''$ Transverse flux magnitude, B_t and orientation are shown by line segments. Grey scale: Continuum intensity. Right: Map of α derived from the vector magnetogram at left. Contours of α in units of $10^{-8}m^{-1}$. Negative α dashed, positive α solid.

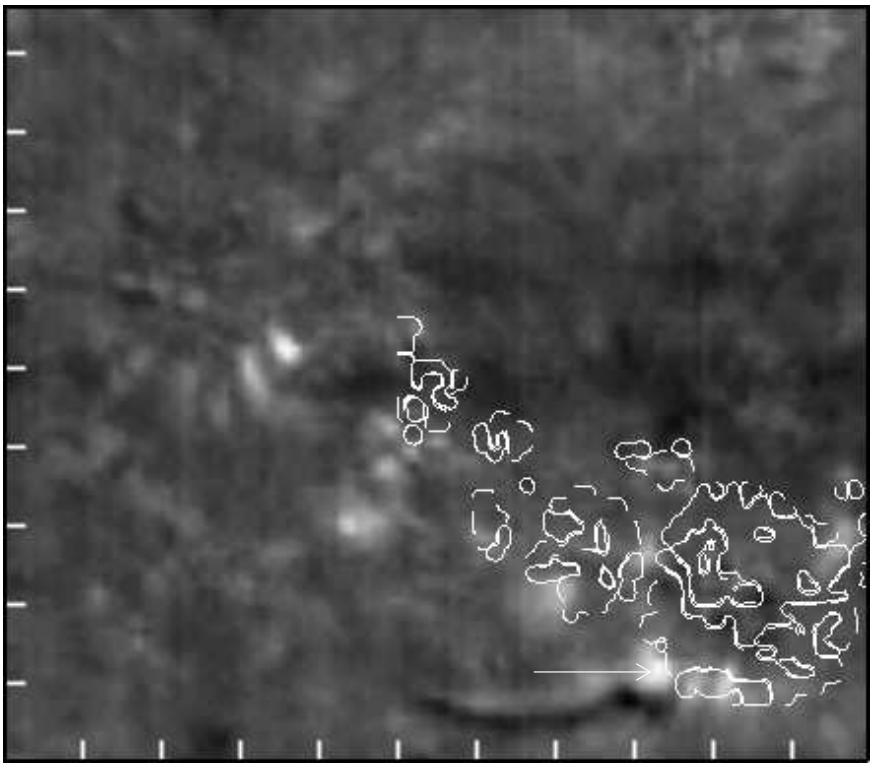

Fig. 4.— MCCD Doppler velocity spectroheliogram overlaid with α contours for AR7117, 1992 March 28. MCCD: 21:57:20 UT, 23.3″ per tick mark. α contours: 21:12:01-22:43:43UT, scaled to same pixel spacing, negative α dashed, positive α solid. Arrow points to origin of surge.

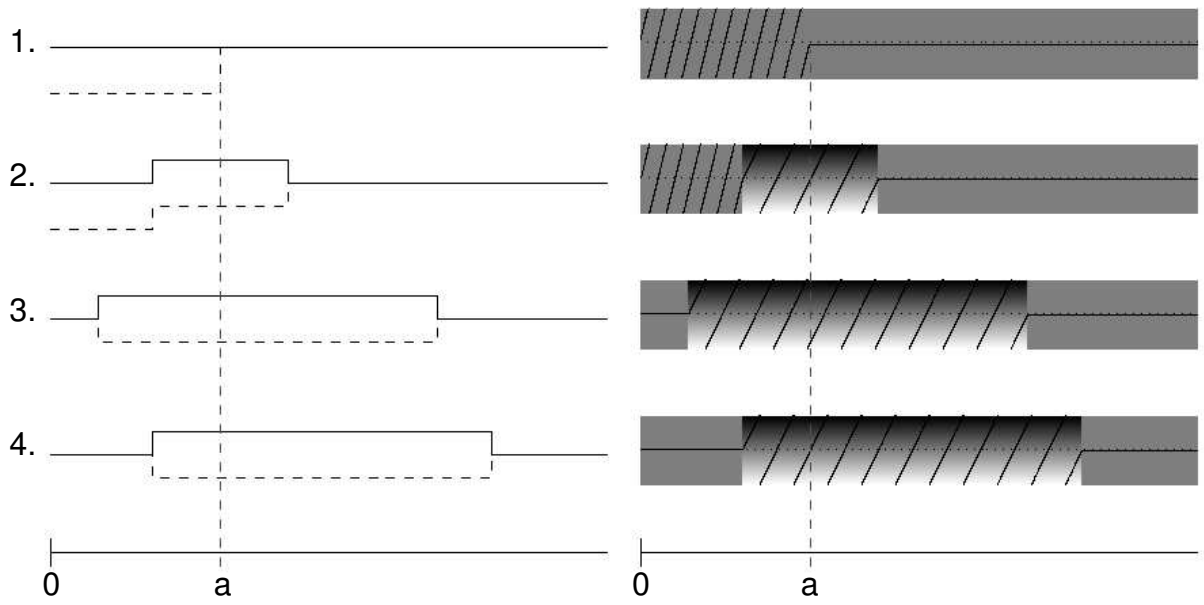

Fig. 5.— Post-reconnection Twist Propagation: Relaxation of left-handed twist in a straight thin flux tube. Left: $d\theta/dz$ dashed, $d\theta/dt$ solid, where θ is defined as the twist around the z-axis. Right: A field line on a relaxing flux tube. $d\theta/dt$ is shown as red or blue shifts with the same convention as the Doppler velocity data and $d\theta/dz$ is shown as twisted lines. Magnetic reconnection takes place at point a at time 1. At instant 2 the surge elongates in both directions until it hits the lower bound where it quits expanding and starts propagating rightward (instant 3). The surge continues propagating rightward at instance 4.

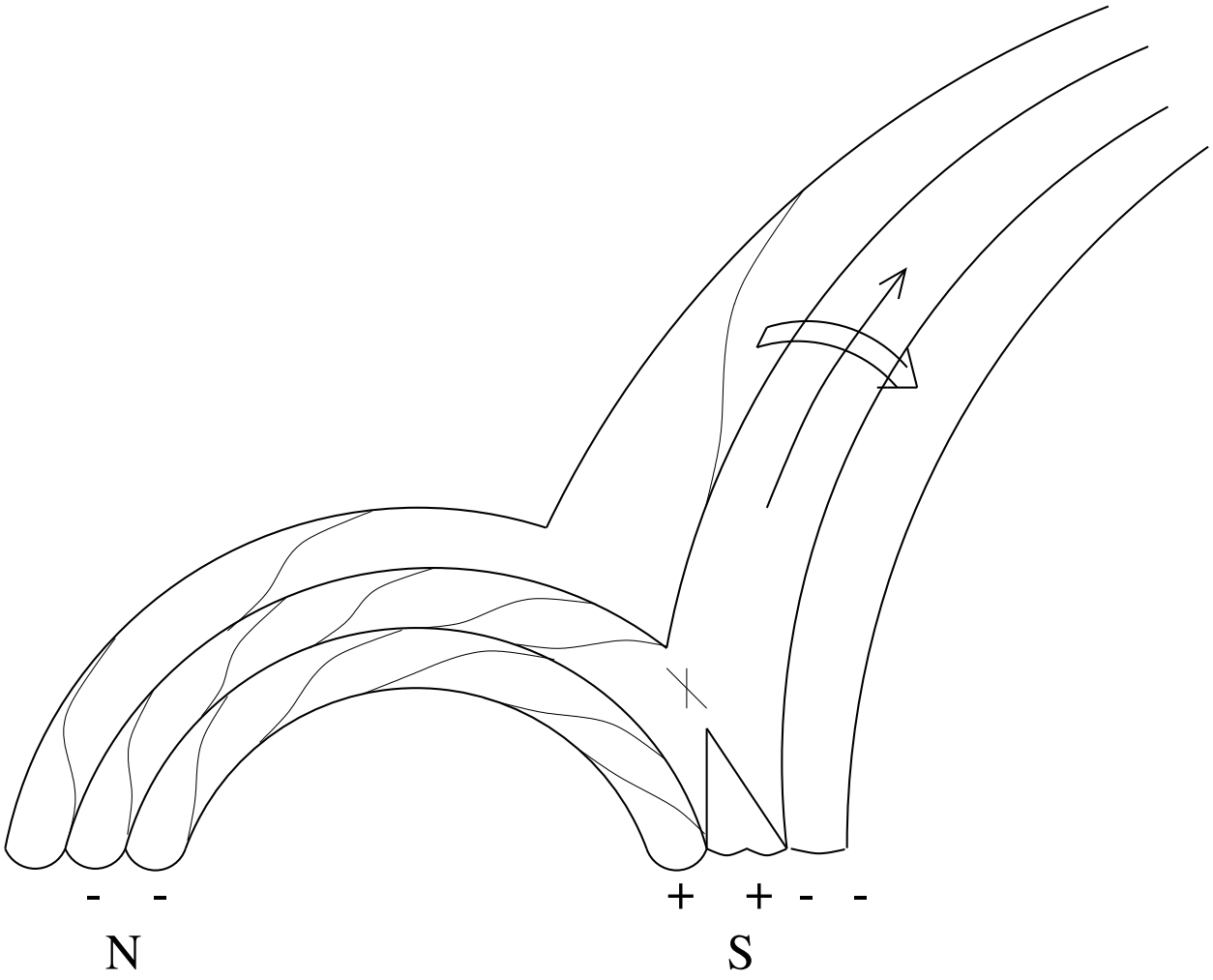

Fig. 6.— Cartoon showing a small twisted (left-handed) dipole reconnecting with untwisted large-scale field at point X. Twist in section N-X goes to large-scale field, that in section S-X goes to small loop formed near S. Arrow above X indicates clockwise motion, as viewed from reconnection site, creating right-handed motion in surge.

Table 1. Active Regions Selected for Study

NOAA	Hem	Date	$\Delta a\%$[a]	Mag	Area (μh)	L	R	?
6891	South	911025	11.1	$\beta\gamma\delta$	2210	1	0	0
		911028	7.7	$\beta\gamma\delta$	2380	0	5	0
		911030	-5.9	$\beta\gamma\delta$	1920	2	4	7
		911031	2.1	$\beta\gamma\delta$	1960	1	0	1
		911101	-24	$\beta\gamma\delta$	1490	0	3	3
7039	South	920207	8.7	$\beta\gamma$	250	2	4	0
		920208	16	$\beta\gamma$	290	1	2	3
7070	North	920222	88.9	$\beta\delta$	510	4	7	4
		920223	37.3	$\beta\delta$	700	2	4	4
7117	North	920325	300	β	240	4	2	0
		920326	129	β	550	3	3	1
		920327	45.5	β	800	1	2	7
		920328	13.8	β	910	6	11	9
		920329	11	β	1010	5	10	16
		920330	15.8	β	1170	12	11	15
		920331	3.4	β	1210	6	0	1
7260	North	920719	10.6	$\beta\gamma\delta$	1040	2	26	12
		920720	25	$\beta\gamma\delta$	1300	4	9	3
7440	South	930305	4.3	$\beta\delta$	730	0	0	1
		930310	-7	$\beta\gamma\delta$	800	2	2	1
		930311	3.8	$\beta\gamma\delta$	830	0	4	1
		930312	-3.6	$\beta\gamma\delta$	800	3	4	6
7515	North	930528	21.1	$\beta\gamma\delta$	230	6	0	2
		930529	17.4	$\beta\gamma\delta$	270	2	0	3
		930530	11.1	$\beta\gamma$	300	0	0	1
7590	North	931001	-11.7	$\beta\gamma\delta$	980	11	13	14
		931002	-9.2	$\beta\gamma\delta$	890	3	6	6
		931003	14.6	$\beta\gamma$	1020	0	4	2
7618	North	931118	13.8	β	740	0	0	0
		931119	1.4	$\beta\delta$	750	0	0	0
		931120	-22.7	$\beta\delta$	580	0	0	0

Table 1—Continued

NOAA	Hem	Date	$\Delta a\%$[a]	Mag	Area (μh)	L	R	?
8179	South	980317	19.4	$\beta\gamma\delta$	800	3	4	5
		980318	-2.5	$\beta\gamma\delta$	780	4	5	3
		980319	1.3	$\beta\gamma\delta$	790	0	5	1
8323	South	980903	16.3	$\beta\gamma\delta$	1430	2	2	8
		980904	2.1	$\beta\gamma\delta$	1460	2	3	6

[a]Percentage of growth or decay of area compared to the previous day

Table 2. Surge Handedness vs Hemisphere

	Surge	Handedness	
Hemisphere	Left	Right	Total
North	71	108	179
South	23	47	70
Total	94	155	249

Table 3. Surge Handedness vs α_{best}

	Surge	Handedness	
α_{best}	Left	Right	Total
Negative	38	74	112
Positive	7	8	15
Total	45	82	127

Table 4. Co-registered Surges Studied

No.	Start(UT)	End(UT)	Surge	Sign of α
7117.80	18:50	19:08	L	+
7117.240	18:48	18:57	R	−
7117.360	21:46	22:23	R	−
7117.890	17:59	18:09	R	−
7117.1060	20:37	21:03	L	+
7117.1220	19:04	19:12	L	+
7260.10	17:05	17:18	R	−[a]
7260.40	17:23	17:38	R	−
7260.50	17:43	17:57	R	−
7260.70	18:00	18:12	R	−
7260.80	18:00	18:21	R	−
7260.90	18:13	18:22	R	+[a]
7260.100	18:24	18:42	R	−
7260.110	18:44	18:54	R	−
7260.120	19:03	19:17	R	+[a]
7260.130	19:17	19:17	R	+
7260.245	21:43	21:47	R	−[a]
7260.260	22:05	22:09	R	+
7260.320	22:40	22:47	R	−[a]
7260.350	23:25	23:30	R	+
7440.120	01:13	01:17	R	−[a]
7440.140	01:44	01:52	R	−[a]
7515.70	22:54	23:05	L	−[a]
8323.10	16:34	16:57	R	−
8323.60	17:41	17:53	L	+
8323.155	17:16	17:52	L	+

[a]Occurred near boundary of sign of α

Table 5. Surge Handedness vs Sign of α at Point of Origin

	Surge	Handedness	
Sign of α	Left	Right	Total
Negative	1	15	16
Positive	5	5	10
Total	6	20	26